FUSION OF ELECTRICAL RESISTIVITY TOMOGRAPHY (ERT) AND RESISTIVITY CONE PENETROMETRY (RCPT) DATA FOR IMPROVED HYDROGEOPHYSICAL CHARACTERISATION

L. M. L. CATT[1], L. J. WEST[1] AND R. A. CLARK[1]

[1] *School of Earth and Environment, University of Leeds, Leeds, LS2 9JT, U.K.*

ABSTRACT

Electrical resistance tomography (ERT) is potentially an appropriate subsurface imaging tool for hydrogeophysical characterisation, due to strong correlations between resistivity and hydrological parameters such as clay content and permeability. However, the ability of ERT to locate accurately sharp boundaries, such as permeability contrasts and wetting fronts, is rather poor because of the relatively large measurement support volume of the technique. This poor ability to locate interfaces also creates problems for ERT applications in geotechnical engineering, where practitioners need accurate determination of lithological interface depths. In contrast, the technique of resistivity cone-penetrometry (RCPT) provides resistivity data with a high vertical resolution, allowing interfaces to be located accurately. However, RCPT bores are usually widely spaced, so horizontal resolution is poor. Hence, combination of RCPT and ERT has significant advantages.

Here, we investigate fusion of ERT and RCPT data for hydrogeophysical characterisation. The ability of RCPT data to guide ERT inversion towards improved solutions is investigated using both synthetic models and field data. A series of synthetic RCPT and Wenner ERT data for a sand body within a clay background was generated. The ERT data were contaminated with 2% and 5% Gaussian noise. A series of reference models for ERT inversion was generated from the synthetic RCPT data. The ERT data were inverted with and without these RCPT-derived reference models. The models produced by inversion (the final models) with the best fit to the original synthetic model were identified. The final models were then ranked using a weighted sum of (i) the least-squares misfit of the original synthetic data to the data produced via forward modelling from the final model, (ii) the least-squares misfit between the final model and the reference model, and (iii) the final model smoothness. This ranking technique identified the same best final models as identified using the best fit to the synthetic model. This result indicates that the reference model approach described here can safely be used with field data, i.e. for an unknown 'true' resistivity distribution. Using RCPT data as a constraint significantly improved interfacial depth accuracy and horizontal boundary location in the final geoelectrical model.

RCPT and ERT data were collected from a coastal site near Withernsea, East Yorkshire, UK, where fluvioglacial sand lenses exist within clay tills. The ERT data were inverted with and without RCPT-derived reference models to produce range of geoelectrical models. These were quantitatively assessed using the procedures identified during the modelling stage. The models were then compared to a logged cliff section. We discuss the implications for the design of combined ERT and RCPT investigations.

1. INTRODUCTION

Sand and gravel bodies within clay-rich tills can alter the engineering properties of a till. They may be water-bearing and can act as groundwater flow conduits. The presence of continuous bodies can lead to shorter groundwater travel times in the till than might otherwise be expected, which has implications for groundwater protection. Such bodies may not be detected or may be incorrectly characterised by conventional investigation techniques (boreholes and trial pits) that acquire high resolution data vertically but tend to be sparse laterally.

Sands and gravels have high resistivities (30Ωm to 225Ωm), while clays have low resistivities (15Ωm to 35Ωm), according to Reynolds, (1996), so Electrical Resistivity Tomography (ERT) is an appropriate detection tool. However, commonly-used ERT inversion routines reconstruct geoelectrical boundaries poorly. This can lead to uncertainty in the dimensions and connectivity of anomalous resistivity bodies. Resistivity Cone Penetrometry (RCPT) provides resistivity data with a high vertical resolution, allowing interfaces to be located accurately. However, RCPT bores are usually widely spaced, so horizontal resolution is poor.

RCPT data and ERT data can be fused in various ways. Inversion routines available for commercial and research purposes such as RES2DINV (Geotomo Software, Penang, Malaysia) and DCINV2D (University of British Columbia Geophysical Inversion Facility) allow the inclusion of a structured initial model (the model from which the inversion starts). DCINV2D also allows the inclusion of a structured reference model (the model which acts as a constraint on the final model). Such models can be informed by RCPT data.

Knight and Pidlisecky (2005) combine ERT and RCPT to image a saltwater plume. An ERT survey was carried out using the fixed subsurface electrodes as current sources. Potentials were measured at the surface and using a mobile electrode mounted on an RCPT probe that also collected RCPT data. The RCPT data informed the initial model for the inversion of the ERT data.

In this study, we concentrate on the use of RCPT data to produce reference models for inversion. For inversion with various reference models derived from RCPT data, we suggest that we can determine which gives the best final model and which give worse final models than inversion with no reference model or a homogenous reference model.

2. THEORY

Previously, we have used synthetic data to assess the influence of reference models (Catt, West and Clark, 2005). A synthetic model of a sand lens in clay was generated, and a synthetic Wenner array field data set produced. These data were contaminated with 50 sets of 2% Gaussian noise and 50 sets of 5% Gaussian noise.

A range of reference models were constructed based on synthetic RCPT data extracted from the original synthetic model. We assumed that the resistivity and top and base of the high resistivity lens were well constrained by RCPT data, while the width was poorly constrained by some other technique, such as an EM survey. Both smooth-and sharp-edged models were constructed. These models were then used in inversion of the noisy synthetic field data. The final resistivity model produced by each inversion was then assessed quantitatively for fit to the original synthetic resistivity model using (i) the l_2 norm of the area-weighted misfit, (ii) the offset of the reconstructed resistivity anomaly centroid from the true resistivity anomaly centroid, and (iii) the difference between the resistivity at the reconstructed resistivity anomaly centroid and the resistivity at the centre of the true resistivity anomaly centroid.

Several attributes were then defined, such as the size and flatness of the final model and the l_2 norm of the area-weighted model misfit between the final model and the reference model. Combinations of these attributes were then assessed to determine whether the inversion with the best reference model could be determined without knowledge of the true resistivity distribution. The cost function R that consistently selected the best final models was found to be the following combination of attributes

$$R = \iint w_d \left(d^{fin} - d^{obs}\right)^2 dxdz + \iint \left(m^{fin} - m^{ref}\right)^2 dxdz + \iint \left(\frac{\partial m^{fin}}{\partial x}\right)^2 + \left(\frac{\partial m^{fin}}{\partial z}\right)^2 dxdz \qquad (1)$$

where d^{obs} are the synthetic data, d^{fin} are the data forward-modelled from the final model m^{fin}, m^{ref} is the reference model and w_d is the data weighting matrix. The noise contaminating the j^{th} observation is assumed to be an uncorrelated Gaussian random variable having zero mean and standard deviation ε_j. w_d is therefore defined as a diagonal matrix having the form $diag\{1/\varepsilon_1 ,\ldots, 1/\varepsilon_j\}$. The first term is the l_2 norm of the data misfit and the second term is the l_2 norm of the area-weighted model misfit. The third term is the horizontal and vertical flatness of the final model; reference models containing smooth and sharp edges were tested and this term forces R to select preferentially smoother final models.

This modelling showed that (i) using a homogenous reference model in inversion can lead to a false negative, i.e. the appearance of no high resistivity lens, (ii) using a reference model that is close to the true resistivity distribution causes the inversion to produce a result that is close to the true resistivity distribution, and (iii) using a reference model that is significantly different to the true resistivity distribution causes the inversion to produce a result that is poor, but does not duplicate the reference model. A paper expanding on these results is in preparation.

3. SURVEY

The field site is near the town of Holmpton, grid reference 537180 424080. The site is near cliffs that provide exposures used for ground-truthing. The geological sequence, based on sections in Berridge and Pattison (1994) and field logs, is illustrated in Figure 1.

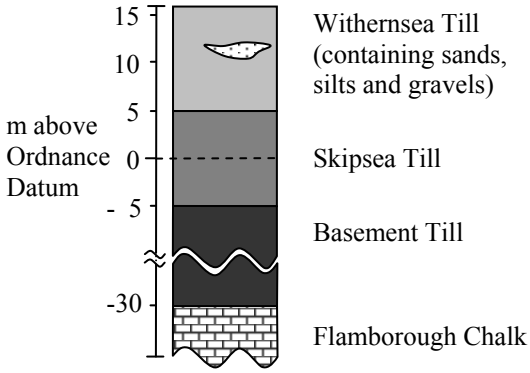

FIGURE 1. Geological sequence at Holmpton.

The survey area layout can be seen in Figure 2. EM and ERT surveys were carried out along seven parallel lines spaced 4m apart and oriented parallel to the edge of the crop. Survey lines ran at an oblique angle to the plough lines in the cropped area and to the cliff face. In this paper we concentrate on processing the first 80m of line 3 of the ERT data, along which the majority of the RCPTs were collected; only the results for this line are presented.

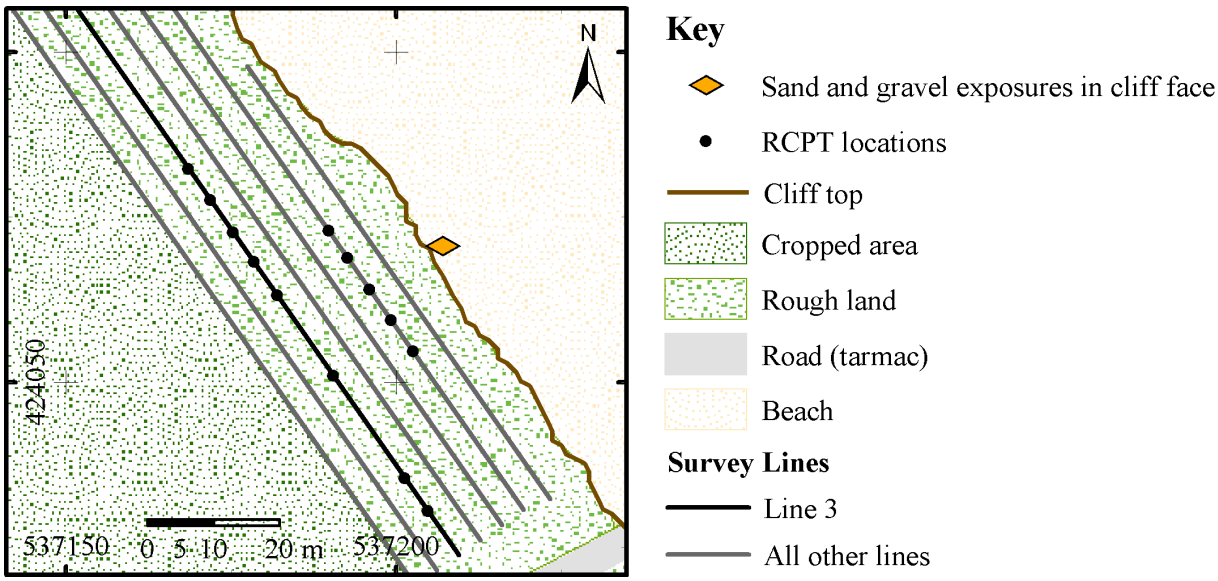

FIGURE 2. Holmpton site plan and survey locations.

ERT and EM data were collected between June and August 2005, during very hot, dry weather. ERT data were collected with an ABEM Lund Terra Meter applying a current of 20mA. The Wenner array with a 2m electrode spacing was used for each line. The maximum number of electrodes available for simultaneous recording was 41, with a 21 electrode roll-on

used for longer lines. Figure 3(a) shows the apparent resistivity pseudosection for the first 80m of line 3.

A Geonics EM-31 was used to take conductivity measurements at every 2m, with the boom oriented at 90° to the survey lines. EM data for line 3 is shown in Figure 3(b).

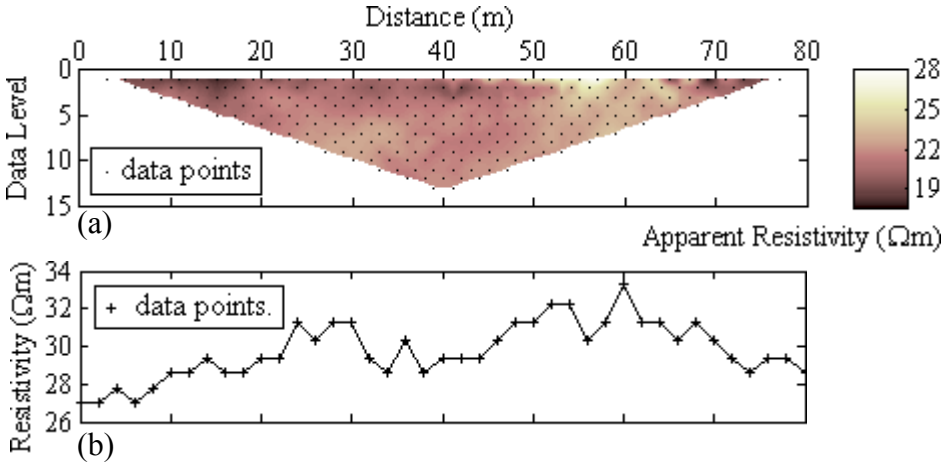

FIGURE 3. Line 3: (a) resistivity pseudosection; (b) EM profile.

RCPT data were collected in January 2006 during very wet, cold conditions. A S15-CFIP.252 cone was used record resistivity to between 9m and 11m depth (see Figure 2 for locations). Line 3 RCPT logs are plotted in Figure 4(a). A model of the resistivity of the subsurface below line 3 was generated from these RCPT data, as shown in Figure 4(b).

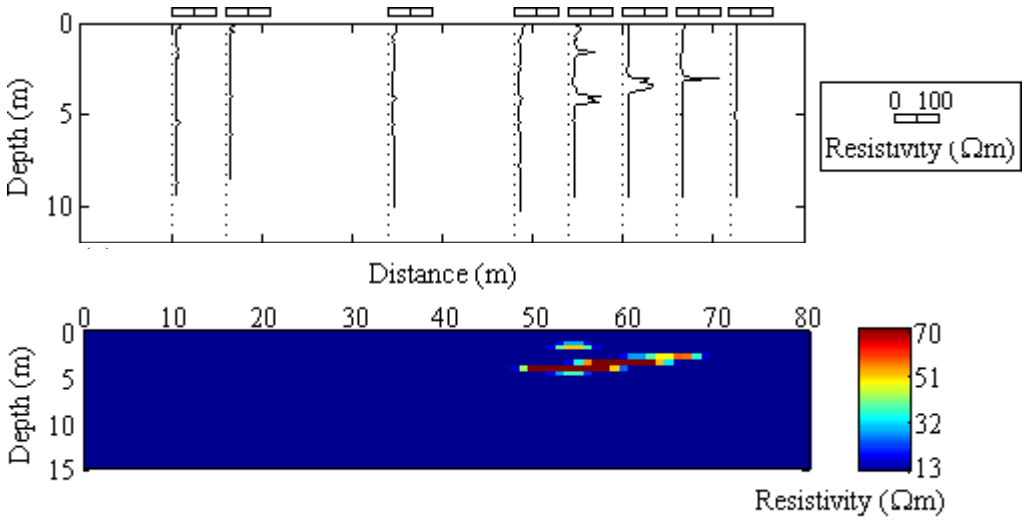

FIGURE 4. Line 3: (a) RCPT logs (2x vertical exageration). Each dotted line is located at the horizontal position of an RCPT and acts as the axis for the resistivity log; (b) RCPT-derived resistivity model.

The ERT data indicate a background resistivity of approximately 20Ωm, whereas the RCPT data indicate a background resistivity of approximately 12Ωm. This is may be due to anisotropy and perhaps differences in soil water content in the top 2m between surveys.

4. ANALYSIS

4.1 Inversion

All inversions were carried out with DCIP2D (Oldenburg and Li, 1994), which allows the use of a structured reference model. In the absence of a user-supplied reference model, the inversion routine calculates a homogenous reference model with a resistivity equal to the mean conductivity of the apparent resistivity data.

4.2 Inversion with a Homogenous Reference Model

The final model produced by inversion using a homogenous reference model is shown in Figure 5. The resistivity section has a broad region of slightly higher resistivity between 22m and 28m, centred on a depth of about 6m (A). The peak resistivity in the anomaly is about 30Ωm, within a background of approximately 20Ωm. It would be easy to conclude from this section there is no consolidated sand and gravel body, or one of only negligible size.

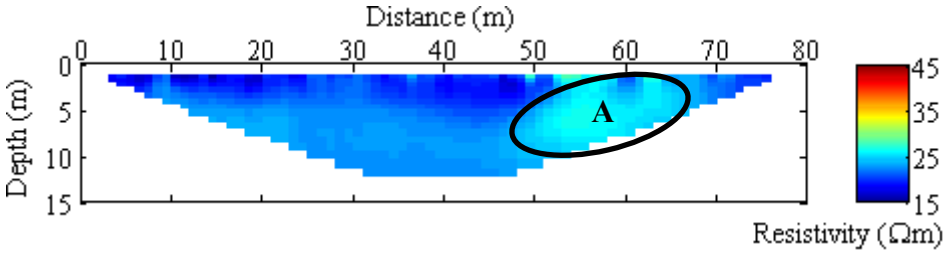

FIGURE 5. Line 3: final model after inversion with a homogenous reference model. See text for significance of **A**.

4.3 Inversions with Reference Models

Twelve reference models containing high-resistivity bodies were generated. Each of three single RCPT logs were used to fix the resistivity and top and base of the bodies; three different body widths were set using the EM-31 data. Six reference models were created with lens-shaped bodies and six with rectangular bodies. Due to the thinness of the lens compared to the size of the inversion mesh cells, a moving-average filter of radius 2.5m was applied to the reference models. Before inversion, 8Ωm was added to all cells in the reference models, in order to correct for the difference in background resistivity observed between the RCPT and ERT surveys (discussed in Section 3).

4.4 Analysis

We assumed that the true model of the resistivity of the subsurface is identical to that in Figure 4(b); this model matches well the shape of a sand and gravel body seen in a cliff exposure (see Figure 2 for location). All models were converted to conductivity (mS/m) before calculations were carried out.

As in the modelling stage, combinations of attributes were assessed to determine whether the best final models could be determined without prior knowledge of the true resistivity distribution. The l_2 norm of the data misfit was not included in these tests as all inversions were set to converge to the same data misfit. First, we calculated the l_2 norm of the area-weighted misfit between the final model and the true model. For each inversion, we then calculated the attribute combination and plotted this against the l_2 norm of the area-weighted misfit between the final model and the true model.

The l_2 norm of the area-weighted misfit between the final model and the reference model succeeded in identifying the best final models. A term to select for smooth models was not needed, as all reference models contained smooth edges. For each inversion, the l_2 norm of the area-weighted misfit of the final model to the reference models is plotted against the l_2 norm of the area-weighted misfit of the final model to the true model (Figure 6). Reference models with lens-shaped and rectangular high-resistivity bodies are grouped to show that the lens-shaped models produce better final models.

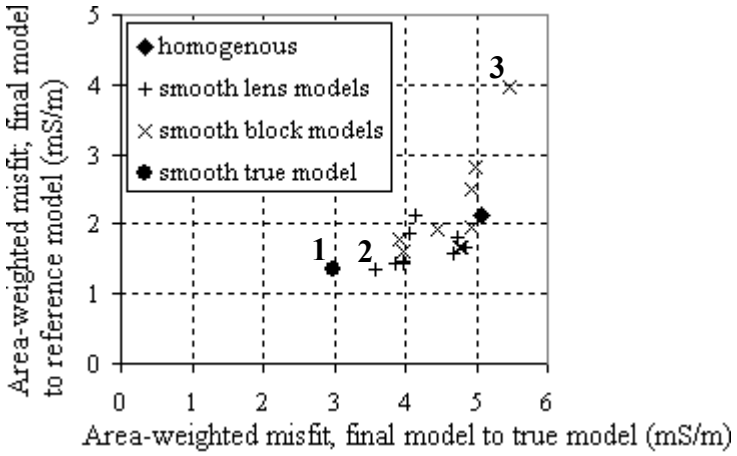

FIGURE 6. Misfit plot. See text for significance of **1**, **2** and **3**.

Figure 7 shows final models with their associated reference models. The models displayed are from inversions using the following reference models: a smoothed true model (1), the best smooth lens model (2), and the worst smooth block model (3). The result of inversion with a homogenous reference model is shown in Figure 5.

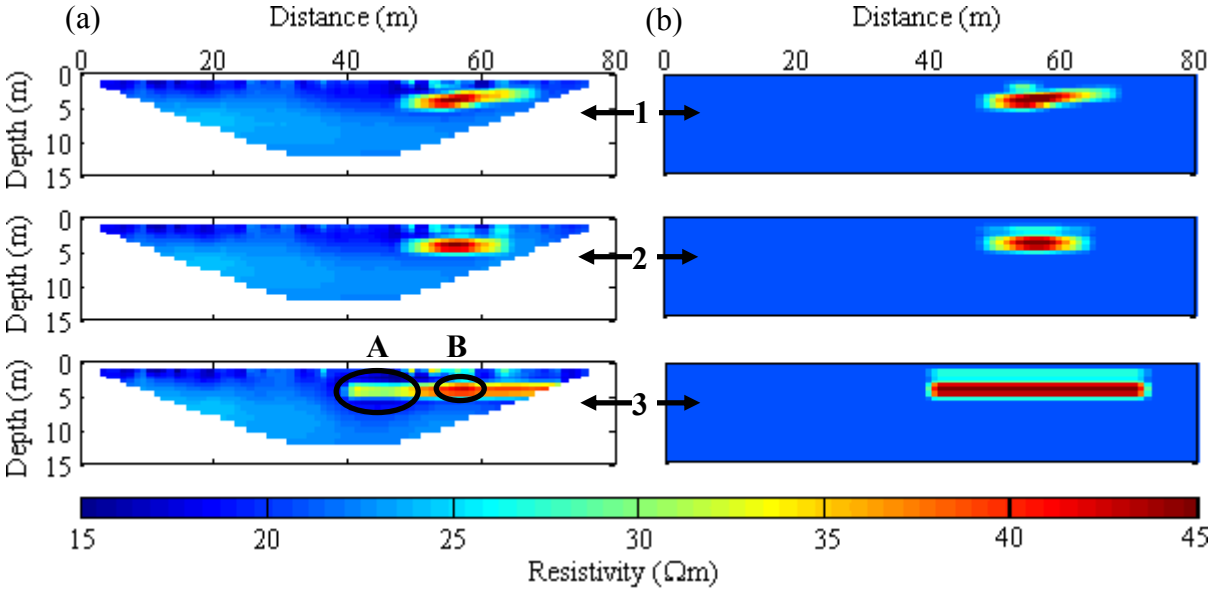

FIGURE 7. Column (a), final models; and column (b) their reference models. See text for significance of **A** and **B.**

Inversions using reference models close to the true model produced final models similar to the reference model (models 1 and 2). Inverting using a poorer reference model produced a final model that retained characteristics of the reference model, but was forced towards the true model; this is seen in model 3 at A where the high resistivity of the reference model has been reduced. It is also seen at B, where there is a resistivity peak. The peak is not present in the reference model, but it is in the same location as the peak resistivity in the true model.

5. CONCLUSION

It has been shown that inverting with a homogenous reference model can lead to final models that underestimate the size and resistivity contrast of small, high resistivity bodies in a low resistivity material. Inverting with a reference model that is close to the true geoelectrical structure of the ground leads to a final model that is close to the true model. When inverting with a poor reference model, the final model is not a reproduction of the reference model; nor is it as close to the true model as the final model produced by inversion with a good reference model. Furthermore, it has been shown that if we invert with a number of reference models, we can identify the best final model without prior knowledge of the true geoelectrical structure. In this way, small, high-resistivity bodies can be identified in ERT survey by using constraining inversion with RCPT data using the reference model approach described here.

This research suggests that a combined ERT and RCPT surveys can offer significant advantages over RCPT or ERT surveys alone.

This research is funded by the Landfill Tax Credit Scheme (LTCS). We thank Keith Mitchell and Mike Haworth of Wardell Armstrong, and Michael Jones of Waste Management Research Ltd. We thank Lankelma Ltd., especially Rob Gardiner, for performing RCPT survey.

REFERENCES

Berridge, N.G., and J. Pattison (1994), *Geology of the country around Grimsby and Patrington, Memoir for 1:50,000 geological sheets 90 and 91 and 81 and 82 (England and Wales)*, British Geological Survey Sheet Memoir, HMSO, London.

Catt, L. M. L., L. J. West, and R. A. Clark (2005), Electrical Resistivity Inversion Constrained by Resistivity Cone Penetrometry (RCPT): Application to Landfill Site Characterisation, *Eos Trans. AGU, 86*(18), Jt. Assem. Suppl., Abstract NS23A-03.

DCIP2D; A Program Library for Forward Modelling and Inversion of DC Resistivity and Induced polarization Data over 2D Structures, version 3.2 (2001). Developed under the consortium research project *Joint/Cooperative Inversion of Geophysical and Geological Data*, UBC-Geophysical Inversion Facility, Department of Earth and Ocean Sciences, University of British Columbia, Vancouver, British Columbia.

Knight, R., and A. Pidlisecky (2005), Cone-Based Geophysical Imaging: a Proposed Solution to a Challenging Problem, *The Leading Edge, 24*(1), 34-38.

Oldenburg, D. W., and Li, Y. (1994), Inversion of Induced Polarization Data, *Geophysics, 59*(9), 1327-1341.

RES2DINV; 2D Resistivity & IP Inversion Software, version 3.55, Geotomo Software, Penang, Malaysia.

Reynolds, J. (1996), *An Introduction to Applied and Environmental Geophysics*, John Wiley & Sons Ltd., Chichester.